Research Article

Uniformly convergent numerical solution for caputo fractional order singularly perturbed delay differential equation using extended cubic B-spline collocation scheme

N.A. Endrie*, and G.F. Duressa

Abstract

This article presents a parameter uniform convergence numerical scheme for solving time fractional order singularly perturbed parabolic convection-diffusion differential equations with a delay. We give a priori bounds on the exact solution and its derivatives obtained through the problem's asymptotic analysis. The Euler's method on a uniform mesh in the time direction

*Corresponding author

Received 16 February 2024; revised 20 May 2024; accepted 27 May 2024

Nuru Ahmed Endrie

Department of Mathematics,College of Natural and Computational Science, Arba Minch University, Arba Minch, Ethiopia. e-mail: nuruahmed222@gmail.com

Gemechis File Duressa

Department of Mathematics, College of Natural and Computational Science, Jimma University, Jimma, Ethiopia. e-mail: gammeef@gmail.com

and the extended cubic B-spline method with a fitted operator on a uniform
mesh in the spatial direction is used to discretize the problem. The fitting
factor is introduced for the term containing the singular perturbation pa-
rameter, and it is obtained from the zeroth-order asymptotic expansion of
the exact solution. The ordinary B-splines are extended into the extended
B-splines. Utilizing the optimization technique, the value of μ (free param-
eter, when the free parameter μ tends to zero the extended cubic B-spline
reduced to convectional cubic B-spline functions) is determined. It is also
demonstrated that this method is better than some existing methods in
the literature.

AMS subject classifications (2020): Primary 65L11; Secondary 65N12.

Keywords: Singularly perturbed problem; Fractional derivative; Artificial
viscosity; Delay differential equation.

1 Introduction

In this work, we consider the singularly perturbed parabolic delay differential
equation of fractional order in time,

$$\mathfrak{L}y(x,t) \equiv D_t^\gamma y(x,t) - \varepsilon\frac{\partial^2 y(x,t)}{\partial x^2} + q(x)\frac{\partial y(x,t)}{\partial x} + r(x,t)y(x,t)$$
$$= -s(x,t)y(x,t-\delta) + f(x,t), \qquad (x,t) \in \Omega = (0,1) \times (0,\mathfrak{T}], (1)$$

with

$$\begin{cases} y(x,t) = \varphi_b(x,t), & \text{for } (x,t) \in [0,1] \times [-\delta,0], \\ y(0,t) = \varphi_l(t), y(1,t) = \varphi_r(t), & \text{for } t \in (0,\mathfrak{T}), \end{cases} \quad (2)$$

where D_t^γ is the Caputo fractional derivative of order $0 < \gamma < 1$, δ is delay
parameter, and $0 < \varepsilon \ll 1$ is the singular perturbation parameter. For the
domain $\bar\Omega = [0,1] \times [0,\mathfrak{T}]$, if

$$q(x) \geq \beta > 0, \quad r(x,t) \geq 0, \quad s(x,t) \geq \alpha > 0,$$

are bounded and smooth functions, then initial data and boundary conditions
are also smooth and bounded in their respective domains. The solution of

---

model problem (1) has a boundary layer of regular type at $x = 1$ with a width of $\mathcal{O}(\varepsilon)$.

Parameter-dependent differential equations, whose solution behavior depends on the magnitude of the parameters, are used to model many physical and biological phenomena. If the highest-order derivative of a differential equation is multiplied by a small positive parameter, $\varepsilon(0 < \varepsilon < 1)$, then the differential equation is said to be singularly perturbed. Such issues arise in modeling of reaction-diffusion processes, chemical reactor theory, aerodynamics, elasticity, quantum mechanics, plasma dynamics, and many other related domains [3].

Fractional calculus has an origin as old as classical calculus, although it was not used for a very long period to solve scientific and engineering problems. Indeed, fractional calculus started attracting the attention of scientists and researchers in recent decades due to its numerous applications [6, 35]. Noninteger derivatives were first introduced by Leibnitz in 1695, as far as the authors can tell.

Derivatives of arbitrary order were mentioned by Euler and Fourier, but no examples or applications were provided. The honor of being the first to apply in real-world scenarios belongs to Niels Henrik Abel [1] in 1823. However, as stated in [6], fractional calculus began to be essential by Riemann and Liouville. Fractional-order differential equations are used to model a wide range of real-world phenomena, including protein dynamics, dielectric relaxation phenomena in polymeric materials, visco-elastic behavior, transport of passive tracers carried by fluid flow in a porous medium in groundwater hydrology, transport dynamics in systems subject to anomalous diffusion, and long-term memory in financial time series [21, 15].

Singularly perturbed delay differential equations (SPDDEs) are employed to model physical problems that evolve based on both their current condition and history. To make a model more realistic, it may be important to represent former system states in addition to the current state. Delay differential equations (DDEs) are useful for describing time-dependent phenomena that rely on a past state [17]. Because delay differential equations have so many applications in the fields, including bio-sciences, control theory, economics, material science, medicine, robotics, and more, there has been a major rise

in interest in studying problems during the past several decades. The field of delay differential equations theory is extensive, with notable works including in [7, 11, 12, 33, 22, 19, 22, 23, 24], and there are various real-world examples of delay differential equations in the works by Nelson and Perelson [32], Villasana and Radunskaya [41], and Zhao [44]. Singularly perturbed problem (SPP) solutions are not smooth and contain boundary layer-related singularities. When the perturbation parameter (ε) and mesh length are lowered, even advanced numerical algorithms do not perform consistently well. The results of classical numerical methods on uniform meshes fail to provide a reasonably accurate approximate solution of the exact solution, and the truncation error becomes unbounded as the singular perturbation parameter tends to zero unless a large number of mesh points are used in the approximation process [13]. However, this highlights the numerical method's computational inefficiency. When the number of mesh points grows, the resulting algebraic system of equations may become ill-conditioned. The shortcoming encourages the creation of a suitable numerical approach whose accuracy is independent of the perturbation parameter, highlighting the key advantage of the proposed method [16].

Xu [43] has proposed the extended cubic B-spline, a generalization of the B-spline. In [42] investigation, the three extended B-splines with degrees 4, 5, and 6 were provided. To modify the shape of the cubic B-spline curve for extended B-splines, a free parameter is added to the cubic B-spline base functions. The degree of the piecewise polynomials is raised, and a one-free parameter is included, but the continuity of the extended cubic B-splines stays in the order of 3. This encourages us to develop an extended cubic B-spline trial function as part of a numerical technique [10]. The spline-based approach has gained a lot of popularity these days among the various algorithms for solving SPDDEs. Daba and Duressa [8] gave a uniform convergent numerical method for the singularly perturbed parabolic convection-diffusion equation with a small delay and advance parameter in the spatial variable of the reaction term using an extended cubic B-spline approach. Additionally, they [9] suggested a uniformly convergent numerical solution based on a cubic B-spline and uniform mesh for this problem. Kumar and Kadalbajoo [26] suggested a parameter-uniform numerical method for the problem using a

cubic B-spline on a Shishkin mesh. Kumar and Kadalbajoo [25] and Negero and Duressa [31] developed a parameter uniform convergent method to solve time-dependent singularly perturbed delay parabolic convection-diffusion initial boundary value problems, respectively, using the cubic B-spline collocation method on a piecewise uniform Shishkine mesh and a uniform mesh. In [18], they devised a fitted extended cubic B-spline collocation method to solve singularly perturbed parabolic equations with nonsmooth convection coefficient and discontinuous source terms.

The numerical solution of time-fractional singularly perturbed ordinary differential equations (ODEs) and partial differential equations (PDEs) has not received much attention in the literature. Bijura [5] presented fractionally ordered nonlinear SPPs using higher-order asymptotic solutions. Using the finite element method, Roop [36] developed the numerical solution of fractional ODEs. Qasem and Muhammed [2] used the Pade approximation to estimate the solution of fractional-order nonlinear singularly perturbed two-point boundary-value problems. The matched asymptotic scheme for fractional-order boundary layer problems has been expanded in [4]. Sayevand and Pichaghchi[39] tackled the fractional order boundary value problem by presenting a method to solve singularly perturbed ODEs. Based on the characteristics of a local fractional derivative, they defined the local fractional derivative and expanded the matching asymptotic expansion approach. A linear B-spline operational matrix of fractional derivatives for singularly perturbed ODEs and PDEs has been proposed in [38]. Sahoo and Vikas [37] devised a finite difference method to address a class of time-fractional singularly perturbed convection-diffusion problems. Kumar and Vigo-Aguiar [27] constructed by discretizing time domains using uniform step size and piece-wise-uniform Shishkin meshes for space domains in the study of delay parabolic and time-fractional SPDEs.

To most of our understanding, there is only one paper in the literature that discusses the construction and analysis of a numerical scheme for the class of SPFODDEs under review [27]. This article aims to present and analyze implicit Euler's scheme for time discretization and spatial discretization based on the extended cubic B-spline method by introducing fitting factors. These

methods yield robust numerical results while preserving important features of the corresponding continuous problems.

This article has been organized into the following sections as follows: The preliminary notions are defined in section 2. In Section 3, the formulation of the continuous problem is discussed along with an analytical solution and an analysis of the derivative behavior using defined bounds. We analyze implicit Euler's scheme for time discretization and spatial discretization based on the extended cubic B-spline method by introducing the fitting factor presented in section 4. Section 5 discusses the uniform convergence analysis of the approach. The numerical experiments carried out to confirm theoretical findings and show the method's accuracy are described in detail in Section 6. An overview of the paper's main conclusions is given in the concluding section.

2 Preliminaries

The definitions and tools needed for this study are provided in this section (see [28, 29, 27]).

Definition 1 (Singularly-perturbed problem)**.** If the highest-order derivative of a differential equation is multiplied by a small parameter ε, where ε is the perturbation parameter and $0 < \varepsilon << 1$, the differential equation is considered singularly perturbed.

Definition 2 (Gamma function)**.** If z is a complex number with a nonnegative real part, then the gamma function $(\mathbb{R}(z) > 0)$ is given by the following definition:
$$\Gamma(z) = \int_0^\infty x^{z-1}e^{-x}dx. \tag{3}$$

Definition 3 (Caputo fractional derivative)**.** For $m \in \mathbb{N}$ and $\gamma \in (m-1, m)$, the Caputo fractional derivative of a function $g(t)$ with lower limit zero is defined as
$$D_0^\gamma g(t) = \frac{1}{\Gamma(m-\gamma)} \int_0^t \frac{g^{(m)}(s)}{(t-s)^{\gamma-m+1}}ds. \tag{4}$$

Definition 4. The function $v(x, t)$ can be defined as the γ-order differentiation, with lower bound zero, of a function $m \in \mathbb{N}$ with regard to t in the

Caputo sense, as follows:

$$\frac{\partial^\gamma v(x,t)}{\partial t^\gamma} = \begin{cases} \frac{1}{\Gamma(m-\gamma)} \int_0^t \frac{\partial^m v(x,s)}{\partial s^m} \frac{1}{(t-s)^{\gamma-m+1}} ds & \text{if } \gamma \in (m-1, m), \\ \frac{\partial^m v(x,t)}{\partial t^m} & \text{if } \gamma = m. \end{cases} \qquad (5)$$

3 Properties of continuous problem

Assuming sufficiently smoothness of $\varphi_l(t), \varphi_r(t),$ and $\varphi_b(x,t)$ and satisfying the following compatibility conditions at the corner points $(0,0),\ (1,0),$ and $(0,-\delta)$ as well as the delay term, the existence and uniqueness of the solution of (1)–(2) can be established. Let

$$\begin{cases} \varphi_b(0,0) = \varphi_l(0), \\ \varphi_b(1,0) = \varphi_r(0), \end{cases} \qquad (6)$$

and

$$\begin{cases} \left.\dfrac{d^\gamma \varphi_l}{d^\gamma t}\right|_{t=0} - \varepsilon \left.\dfrac{\partial^2 \varphi_b}{\partial x^2}\right|_{(0,0)} + q(0) \left.\dfrac{\partial \varphi_b}{\partial x}\right|_{(0,0)} + r(0,0)\varphi_b(0,0) \\ \qquad = -s(0,0)\varphi_b(0,-\delta) + f(0,0), \\ \\ \left.\dfrac{d^\gamma \varphi_l}{d^\gamma t}\right|_{t=0} - \varepsilon \left.\dfrac{\partial^2 \varphi_b}{\partial x^2}\right|_{(1,0)} + q(1) \left.\dfrac{\partial \varphi_b}{\partial x}\right|_{(1,0)} + r(1,0)\varphi_b(1,0) \\ \qquad = -s(1,0)\varphi_b(0,-\delta) + f(1,0). \end{cases} \qquad (7)$$

The reduced problem obtained by putting $\varepsilon = 0$ in (1) is

$$D_t^\gamma y(x,t) + q(x)\frac{\partial y(x,t)}{\partial x} + r(x,t)y(x,t) = -s(x,t)y(x,t-\delta) + f(x,t),$$
$$(x,t) \in \Omega. \qquad (8)$$

This is a hyperbolic partial differential equation of first order. Because (8) contains first-order derivatives, the reduced problem is not required to meet the boundary conditions. Thus, the solution to the problem in (1) displays a boundary layer.

Now, we will show that the operator $\mathfrak{L}$ satisfies the maximum principle.

Lemma 1 (Continuous maximum principle)**.** Consider the function $\phi(x,t) \in C^2(\Omega) \cap C^0(\bar{\Omega})$, with $\mathfrak{L}\phi(x,t) \geq 0$ in Ω and $\phi(x,t) \geq 0$, for all $(x,t) \in \Lambda = \{0\} \times (0,\mathfrak{T}] \cup \{1\} \times (0,\mathfrak{T}] \cup [0,1] \times [-\delta,0]$. Then $\phi(x,t) \geq 0$, for all $(x,t) \in \bar{\Omega}$.

Proof. Let us assume that there exists $(\varsigma,\iota) \in \bar{\Omega}$ with

$$\phi(\varsigma,\iota) = \min_{(x,t)\in\bar{\Omega}} \phi(x,t), \quad \text{and} \quad \phi(\varsigma,\iota) < 0.$$

Based on this assumptions, one may confirm that $(\varsigma,\iota) \notin \Lambda$, which implies that $(\varsigma,\iota) \in \Omega$. Using the operator $\mathfrak{L}$ on $\phi(x,t)$, we get

$$\mathfrak{L}\phi(x,t) = D_t^\gamma \phi(x,t) - \varepsilon\phi_{xx}(x,t) + q(x)\phi_x(x,t) + r(x,t)\phi(x,t).$$

At the point of minimum (ς,ι), we obtain

$$\mathfrak{L}\psi((\varsigma,\iota)) = D_t^\gamma \phi(\varsigma,\iota) - \varepsilon\phi_{xx}(\varsigma,\iota) + q(\varsigma)\phi_x(\varsigma,\iota) + r(\varsigma,\iota)\psi(\varsigma,\iota).$$

The function ϕ has minimum at the point (ς,ι), so $D_t^\gamma \phi \geq 0$, $\phi_x = 0$, $\phi_{xx} \geq 0$ at point (ς,ι), and $r(\varsigma,\iota) \geq 0$ for $(\varsigma,\iota) \in \Omega$. Therefore, we have

$$\mathfrak{L}\psi(\varsigma,\iota) < 0.$$

This contradicts our assumption $\mathfrak{L}\phi(x,t)$ in Ω.

Thus, we conclude that $\phi(x,t) \geq 0$, for all $(x,t) \in \bar{\Omega}$. $\qquad\square$

Lemma 2. The differential equation (1)–(2) has a solution $y(x,t)$ that satisfies this estimate:

$$|y(x,t) - \varphi_b(x,0)| \leq Ct, \qquad (x,t) \in \bar{\Omega},$$

in which C is a constant that does not depend on ε.

Proof. See reference [30]. $\qquad\square$

Lemma 3. With its initial and boundary conditions in (2), the solution to problem (1) is bounded as follows:

$$|y(x,t)| \leq C, \quad \text{for all } (x,t) \in \bar{\Omega}. \tag{9}$$

Proof. From Lemma 2

$$|y(x,t)| = |y(x,t) - \varphi_b(x,0) + \varphi_b(x,0)|$$
$$\leq |y(x,t) - \varphi_b(x,0)| + |\varphi_b(x,0)|$$
$$\leq Ct + |\varphi_b(x,0)|$$
$$\leq Ct + C$$
$$\leq C \qquad \text{since } t \in (0, \mathfrak{T}], \ t \text{ is bounded.}$$

$\square$

4 Numerical schemes

We are going to develop the numerical scheme in this section as well. After discretizing the temporal derivative using implicit Euler's scheme, we discretize the spatial derivative based on the extended cubic B-spline approach by applying a fitting factor on a uniform mesh to solve the resulting system of ordinary differential equations.

4.1 Temporal discretization

We first partition the time domain $[0, \mathfrak{T}]$ into M_τ subintervals having uniform step size $\tau = \mathfrak{T}/M_\tau$. We chose M_τ so that for some positive integer $k \in (0, M_\tau)$, $\delta = k\tau$ needs to be a mesh point. A collection of all mesh points in the time direction is represented by the set Ω^{M_τ}; we then have $\Omega^{M_\tau} = \{t_0 = 0 < t_1 < t_2 < \cdots < t_k = \delta < t_{M_\tau - 1} < t_{M_\tau} = \mathfrak{T}\}$. We employ $\Omega_\delta^{M_\tau}$ as the collection of all mesh points between zero and $-\delta$; $\Omega_\delta^{M_\tau} = \{t_{-k} = -\delta < t_{-k+1} < \cdots < t_{-1} < t_0 = 0\}$.

According to Definition 4,

$$z(x, t_{j+1}) = \frac{\partial^\gamma y(x, t_{j+1})}{\partial t^\gamma}$$
$$= \frac{1}{\Gamma(1-\gamma)} \int_0^{t_{j+1}} \frac{\partial y(x, t_{j+1})}{\partial t} (t_{j+1} - \eta)^{-\gamma} d\eta$$
$$= \frac{\tau)^{-\gamma}}{\Gamma(2-\gamma)} \sum_{i=0}^{j} B_i \left(y(x, t_{j-i+1}) - y(x, t_{j-i}) \right) + \mathcal{R}_\tau$$

$$= \sigma \sum_{i=0}^{j} B_i \left(y(x, t_{j-i+1}) - y(x, t_{j-i}) \right) + \mathcal{R}_\tau$$

$$= \sigma y(x, t_{j+1}) - \sigma y(x, t_{j+1}) \sigma \sum_{i=1}^{j} B_i \left(y(x, t_{j-i+1}) - y(x, t_{j-i}) \right) + \mathcal{R}_\tau,$$

where

$$\mathcal{R}_\tau = O(\tau) \int_0^{t_{j+1}} (t_{j+1} - \eta)^{-\gamma} d\eta \quad \text{is} \quad \text{the} \quad \text{truncation} \quad \text{error,}$$

and

$$\sigma = \frac{\tau)^{-\gamma}}{\Gamma(2 - \gamma)}, \quad B_i = (i+1)^{1-\gamma} - (i)^{1-\gamma}.$$

Hence we obtain

$$z(x, t_{j+1}) = \sigma y(x, t_{j+1}) - \sigma y(x, t_j) + \sigma \sum_{i=1}^{j} B_i \left(y(x, t_{j-i+1}) - y(x, t_{j-i}) \right) + \mathcal{R}_\tau. \tag{10}$$

Substituting (10) into (1) On Ω^{M_τ}, we get

$$z(x, t_{j+1}) - \varepsilon \frac{\partial^2 y^{j+1}(x)}{\partial x^2} + q(x) \frac{\partial y^{j+1}(x)}{\partial x} + r^{j+1}(x) y^{j+1}(x)$$
$$= -s^{j+1}(x) y^{j-k+1}(x) + f^{j+1}(x).$$

Once the expressions are rearranged and the operator form has been put in, we get

$$\tilde{\mathfrak{L}} y^{j+1}(x) = -\varepsilon \frac{\partial^2 y^{j+1}(x)}{\partial x^2} + q(x) \frac{\partial y^{j+1}(x)}{\partial x} + \nu^{j+1}(x) y^{j+1}(x) = F^j(x) \tag{11}$$

for $j = 1, 2, \ldots, M_\tau$ with

$$\begin{cases} y(x, t) = \varphi_b(x, t_j), & \text{for} (x, t) \in [0, 1] \times [-\delta, 0], \\ y(0, t_j) = \varphi_l(t_j), y(1, t_j) = \varphi_r(t_j), & \text{for} \ \ t \in (0, \mathfrak{T}), \end{cases} \tag{12}$$

where

$$\nu(x, t_{j+1}) = r^{j+1}(x) + \sigma,$$

$$F^{j+1}(x) = \begin{cases} -s^{j+1}(x)\varphi_b(x, t_{j-k+1}) + f(x, t_{j+1}) + \sigma B_j \varphi_b(x, t_j) \\ +\sigma \sum_{i=1}^{j} B_i \left(y(x, t_{j-i+1}) - y(x, t_{j-i}) \right), \quad \text{for } j = 1, 2, \ldots, k, \\ \\ -s^{j+1}(x)y^{j-k+1}(x) + f^{j+1}(x) + \sigma \psi_b(x, t_j) \\ +\sigma \sum_{i=1}^{j} B_i \left(y(x, t_{j-i+1}) - y(x, t_{j-i}) \right), \quad \text{for } j = k+1, \ldots, M_\tau. \end{cases}$$

After some rearrangement of (11) we obtain

$$\left(1 + \alpha_0 \mathfrak{L}_{\varepsilon, \delta}^* \right) y^{j+1}(x) = F^{j+1}(x), \tag{13}$$

where

$$\alpha_0 = \Gamma(2 - \gamma)\Delta t^\gamma,$$

$$\mathfrak{L}_{\varepsilon, \delta}^* = -\varepsilon \frac{\partial^2}{\partial x^2} + q(x)\frac{\partial}{\partial x} + r^{j+1}(x),$$

$$F^{j+1}(x) = \begin{cases} -\alpha_0 r^{j+1}(x)\varphi_b(x, t_{j-k+1}) + \alpha_0 f j + 1(x) + \varphi_b(x, t_j) \\ +\sum_{i=1}^{j} B_i \left(y(x, t_{j-i+1}) - y(x, t_{j-i}) \right), \quad \text{for } j = 1, 2, \ldots, k, \\ \\ -\alpha_0 r^{j+1}(x)y^{j-k+1}(x) + \alpha_0 f j + 1(x) + \varphi_b(x, t_j) \\ +\sum_{i=1}^{j} B_i \left(y(x, t_{j-i+1}) - y(x, t_{j-i}) \right), \quad \text{for } j = k+1, \ldots, M_\tau. \end{cases}$$

Lemma 4 (Semi-discrete Maximum Principle). Let $\psi(x, t_{j+1})$ be a smooth function such that $\psi(x, t_{j+1}) \geq 0$ and, $\psi(x, t_{j+1}) \geq 0$, for all $(x, t_{j+1}) \in \Lambda = \{0\} \times (0, \mathfrak{T}] \cup \{1\} \times (0, \mathfrak{T}] \cup [0, 1] \times [-\delta, 0]$. Then $(1 + \mathfrak{L}_{\varepsilon, \delta}^*)\psi(x, t_{j+1}) \geq 0$ in $\tilde{\Omega}$ implies that $\psi(x, t_{j+1}) \geq 0$, for all $(x, t_{j+1}) \in \bar{\Omega}$.

Proof. Suppose that there exists $(\iota, t_{j+1}) \in \bar{\Omega}$ with

$$\psi(\iota, t_{j+1}) = \min_{(x, t_{j+1}) \in \bar{\Omega}} \psi(x, t_{j+1}), \quad \text{and} \quad \psi(\iota, t_{j+1}) < 0,$$

and that $\psi(\iota, t_{j+1}) < 0$. Then

$$(\iota, t_{j+1}) \notin \{(0, t_{j+1}), (1, t_{j+1})\} \quad \text{and} \quad \psi_x(\iota, t_{j+1}) = 0, \psi_{xx}(\iota, t_{j+1}) > 0.$$

Applying the operator $\mathfrak{L}_{\varepsilon, \delta}^*$ on $\psi(x, t_{j+1})$, we get

$$(1 + \alpha_0 \mathfrak{L}_{\varepsilon, \delta}^*)\psi(x, t_{j+1}) = \psi(\iota, t_{j+1}) + \alpha_0 \left(-\varepsilon \psi_{xx}(x, t_{j+1}) + q(x)\psi_x(x, t_{j+1}) \right.$$

$$+ r(x, t_{j+1})\psi(x, t_{j+1})) .$$

At the point of minimum (ι, t_{j+1}), we obtain

$$(1 + \alpha_0 \mathfrak{L}^*_{\varepsilon,\delta})\psi(\iota, t_{j+1}) = \psi(\iota, t_{j+1}) + \alpha_0(-\varepsilon\psi_{xx}(\iota, t_{j+1}) + q(\iota)\varphi_x(\iota, t_{j+1})$$
$$+ r(\iota, t_{j+1})\psi(\iota, t_{j+1})).$$

At the point (ι, t_{j+1}), the function ψ has minimum, so $\psi_x = 0$, $\psi_{xx} \geq 0$ at point (ι, t_{j+1}) and $r(\iota, t_{j+1}) \geq 0$ for $(\iota, t_{j+1}) \in \Omega$. Therefore, we have

$$(1 + \alpha_0 \mathfrak{L}^*_{\varepsilon,\delta})\psi(\iota, t_{j+1}) < 0,$$

which contradicts our assumption $(1 + \mathfrak{L}^*_{\varepsilon,\delta})\psi(x, t_{j+1})$ in Ω.

Therefore, we conclude that $\psi(x, t_{j+1}) \geq 0,$ for all $(x, t_{j+1}) \in \bar{\Omega}$.

Hence from the above prove the operator $(1 + \alpha_0 \mathfrak{L}^*_{\varepsilon,\delta})$ satisfies the maximum principle, and consequently

$$\left\| (1 + \alpha_0 \mathfrak{L}^*_{\varepsilon,\delta})^{-1} \right\| \leq \frac{1}{1 + \theta\tau}. \tag{14}$$

$$\square$$

Lemma 5. [Truncation error] The local truncation error corresponding to the semi-discretized problem (12) satisfies

$$\left| \mathcal{R}^{j+1}_\tau \right| \leq C\tau^{2-\gamma}. \tag{15}$$

Proof. From semi-discretized problem, we have

$$\begin{aligned}
\mathcal{R}^{j+1}_\tau &= \frac{O(\tau)}{\Gamma(1-\gamma)} \int_0^{t_{j+1}} (t_{j+1} - \eta)^{-\gamma} d\eta \\
&= \frac{O(\tau)}{\Gamma(1-\gamma)} \int_0^{(j+1)\tau} ((j+1)\tau - \eta)^{-\gamma} d\eta \\
&= \frac{O(\tau)}{\Gamma(1-\gamma)} \frac{((j+1)\tau)^{1-\tau}}{1-\gamma} \\
&= \frac{((j+1)\tau)^{1-\tau}}{\Gamma(2-\gamma)} O(\tau)(\tau^{1-\tau}) \\
&\leq \frac{((j+1)\tau)^{1-\tau}}{\Gamma(2-\gamma)} \tau^{2-\tau} \\
&\leq C\tau^{2-\tau}.
\end{aligned}$$

Therefore, we obtain

$$\left|\mathcal{R}_\tau^{j+1}\right| \leq C\tau^{2-\tau}.$$

$\square$

Lemma 6. [Global error bound:] The global error estimation at t_{j+1} satisfies

$$\|E_{j+1}\| \leq C\tau^{2-\gamma}.$$

Proof. Since the function $y(x, t_{j+1})$ satisfies

$$(1 + \alpha_0 \mathfrak{L}_{\varepsilon,\delta}^*)y(x, t_{j+1}) = F^{j+1}(x), \tag{16}$$

and also the solution of the continuous problem (1)–(2) is smooth enough, then we have

$$\begin{aligned} F^{j+1}(x) &= (1 + \alpha_0 \mathfrak{L}_{\varepsilon,\delta}^*)y(x, t_{j+1}) + \mathcal{R}_\tau^{j+1} \\ &= (1 + \alpha_0 \mathfrak{L}_{\varepsilon,\delta}^*)y(x, t_{j+1}) + C\tau^{2-\gamma}, \end{aligned} \tag{17}$$

From (16)–(17), the error corresponding to (13) satisfies the following boundary value problem:

$$\begin{aligned} (1 + \alpha_0 \mathfrak{L}_{\varepsilon,\delta}^*)E_{j+1} &= C\tau^{2-\gamma}, \\ \implies E_{j+1} &= (1 + \alpha_0 \mathfrak{L}_{\varepsilon,\delta}^*)^{-1}\tau^{2-\gamma}, \end{aligned}$$

$$\|E_{j+1}\| \leq \frac{1}{1 + \theta\tau}C\tau^{2-\gamma}.$$

hence, we obtain the result

$$\|E_{j+1}\| \leq C\tau^{2-\gamma}.$$

$\square$

Theorem 1. The semi-discretize solution $y(x, t_{j+1})$ and its derivatives satisfy the following bounds:

$$\left|\frac{d^i y(x, t_{j+1})}{dx^i}\right| \leq C(1 + \varepsilon^{-i}\exp(-\beta(1 - x)/\varepsilon)), \qquad \text{for} \quad i = 0, 1, 2, 3, 4.$$

Proof. For the proof, refer [14]. $\square$

We can write (11) as operator form,

$$\tilde{\mathfrak{L}}_\varepsilon^\tau y^{j+1}(x) = F^j(x), \tag{18}$$

where $\tilde{\mathfrak{L}}_\varepsilon^\tau y(x) = -\varepsilon \frac{\partial^2 y(x)}{\partial x^2} + q(x)\frac{\partial y(x)}{\partial x} + \nu(x)y(x)$ and

$$F^j(x) = \begin{cases} -s^{j+1}(x)\varphi_b(x,t_{j-k+1}) + f(x,t_{j+1}) + \sigma B_j \varphi_b(x,t_j) \\ +\sigma \sum_{i=1}^j B_i \left(y(x,t_{j-i+1}) - y(x,t_{j-i}) \right), \qquad \text{for } j = 1,2,\ldots,k, \\ \\ -s^{j+1}(x)yj - k + 1(x) + f^{j+1}(x) + \sigma\psi_b(x,t_j) \\ +\sigma \sum_{i=1}^j B_i \left(y(x,t_{j-i+1}) - y(x,t_{j-i}) \right), \qquad \text{for } j = k+1,\ldots,M_\tau. \end{cases}$$

4.2 Spatial discretization

To solve the semi-discretized problem (11), we use the extended cubic B-spline collocation scheme. To take into consideration the exponential properties of exact solution on the uniform mesh, artificial viscosity will be introduced. Thus, an artificial viscosity $\sigma(x,\varepsilon)$ replaces the perturbation parameter ε, which disrupts the highest derivative.

4.3 Extended cubic B-spline collocation method

We divided the spatial domain using uniform mesh such that the set $\Omega_x^{N_h}$ is the collection of all mesh points in the spacial direction; with $x_i = ih$, $i = 0,1,2,\ldots,N_h$.

The extended cubic B-spline G_i of degree 4 for $\mu \in (-8,1)$, has the following form [10]:

$$
G_i(x) = \frac{1}{24h^4}
\begin{cases}
4h(1-\mu)(x-x_i)^3 + 3\mu(x-x_{i-2})^4, & x \in [x_{i-1}, x_{i-1}], \\[2em]
\begin{aligned}
&(4-\mu)h^4 + 12h^3(x-x_{i-1}) + 6h^2(2+\mu)(x-x_{i-1})^2 \\
&-12h(x-x_{i-1})^3 - 3\mu(x-x_{i-1})^4,
\end{aligned} & x \in [x_{i-1}, x_i], \\[2em]
\begin{aligned}
&(4-\mu)h^4 + 12h^3(x_{i+1}-x) + 6h^2(2+\mu)(x_{i+1}-x)^2 \\
&-12h(x_{i+1}-x)^3 - 3\mu(x_{i+1}-x)^4,
\end{aligned} & x \in [x_i, x_{i+1}], \\[2em]
4h(1-\mu)(x_{i+2}-x)^3 + 3\mu(x_{i+2}-x)^4, & x \in [x_{i+1}, x_{i+2}], \\[2em]
0, & \text{otherwise.}
\end{cases}
\tag{19}
$$

Consider that the approximation y_i to the exact solution $Y(x,\mu)$ at the point (x, t_{j+1}). It can be defined as follows using combinations of the cubic B-splines and unknown time-dependent parameters:

$$
Y(x,\mu) = \sum_{k=-1}^{N_h+1} a_k G_k,
\tag{20}
$$

where a_k are time dependent parameters to be determined from the collocation method with the boundary and initial conditions.

Outside of the region $[x_{i-1}, x_{i+2}]$, the extended cubic B-splines and their four principle derivatives vanish. Principle four spline functions cover the interval $[x_{i-1}, x_i]$. Thus, the $y(x,t)$ variation over the element can be written as

$$
Y(x,\mu) = \sum_{k=i-1}^{i+2} a_k G_k,
\tag{21}
$$

where a_{i-1}, a_i, a_{i+1}, and a_{i+2} are the element parameters. Equation (21) can be used to compute the values of the cubic B-spline $G_k(x,\mu)$ and its successive derivatives $G_k'(x,\mu), G_k''(x,\mu)$ at the knots. These values are provided in Table 1 below.

Table 1: Values of $G_k(x, \mu)$ and its principle two derivatives at the node points

G_i	x_{i-2}	x_{i-1}	x_i	x_{i+1}	x_{i+1}
$G_i(x_i, \mu)$	0	$\frac{4-\mu}{12}$	$\frac{8+\mu}{12}$	$\frac{4-\mu}{24}$	0
$G_i'(x_i, \mu)$	0	$-\frac{1}{2h}$	0	$\frac{1}{2h}$	0
$G_i''(x_i, \mu)$	0	$\frac{2+\mu}{2h^2}$	$-\frac{2+\mu}{h^2}$	$\frac{2+\mu}{2h^2}$	0

Substituting the values of Table 1 in (11) and its first and second derivatives at node x_i gives

$$
\begin{aligned}
y(x_i, \mu) &= \frac{4-\mu}{24}a_{i-1} + \frac{8+\mu}{12}a_i + \frac{4-\mu}{24}a_{i+1}, \\
y'(x_i, \mu) &= -\frac{1}{2h}a_{i-1} + \frac{1}{2h}a_{i+1}, \\
y''(x_i, \mu) &= \frac{2+\mu}{2h^2}a_{i-1} - \frac{2+\mu}{h^2}a_i + \frac{2+\mu}{2h^2}a_{i+1}.
\end{aligned}
\tag{22}
$$

Substituting (22) into (11), then we obtain

$$
\begin{aligned}
&-\frac{\xi(i)(2+\mu)}{2h^2}\left(a_{i-1} - 2a_i + a_{i+1}\right) - \frac{q_i}{2h}\left(a_{i-1} - a_{i+1}\right) \\
&+ \nu_i^{j+1}\left(\frac{4-\mu}{24}a_{i-1} + \frac{8+\mu}{12}a_i + \frac{4-\mu}{24}a_{i+1}\right) = F_i^j.
\end{aligned}
\tag{23}
$$

Let us introduce the artificial viscosity $\xi(x_i, \varepsilon)$ into (11). Artificial diffusion (or artificial viscosity) is added to the term in the given differential equation that contains the singular perturbation parameter to generate the discretization scheme. This artificial diffusion is introduced by means of fitting factor $\xi_i(\varepsilon) = \xi(x_i, \varepsilon)$. The zero order asymptotic solution of (18) exists and unique (see [29, 34]) given as

$$
y(x) = y_0(x) + [\varphi_r - y_0(1)]\exp\left(-\int_0^1\left(\frac{q(x)}{\varepsilon} - \frac{r(x)}{q(x)}\right)dx\right) + O(\varepsilon). \tag{24}
$$

Approximation for $q(x)$ and $r(x)$ confined to their first terms about $x = 1$ from Taylor's series can be obtained as

$$
y(x) = y_0(x) + [\varphi_r - y_0(1)]\exp\left(-\frac{q(x)(1-x)}{\varepsilon}\right), \tag{25}
$$

where $y_0(x)$ is the solution of the reduced problem. The convection-diffusion problem in (2) has a right layer, and we have the uniform discretization

point $x_i = ih$ and $\rho = \frac{h}{\varepsilon}$. By taking the limit $h \longrightarrow 0$, for (25) at x_{i-1}, x_i and x_{i+1}, then we obtain

$$
\begin{aligned}
\lim_{h \to 0} y_i &= y_0(0) + [\varphi_r - y_0(1)] \, e^{-\frac{q(x)}{\varepsilon}(1-x)}, \\
\lim_{h \to 0} y_{i-1} &= y_0(0) + [\varphi_r - y_0(1)] \, e^{-\frac{q(x)}{\varepsilon}(1-x)} e^{-q(0)\rho}, \\
\lim_{h \to 0} y_{i+1} &= y_0(0) + [\varphi_r - y_0(1)] \, e^{-\frac{q(x)}{\varepsilon}(1-x)} e^{q(0)\rho}.
\end{aligned}
\tag{26}
$$

Now, we determine the fitting factor ξ by considering the fitted operator (18); that is,

$$
\lim_{h \to 0} \xi_i = \lim_{h \to 0} \frac{q(i)}{2+\mu} \left(\frac{a_{i-1} - a_{i+1}}{a_{i-1} - 2a_i + a_{i+1}} \right). \tag{27}
$$

By substituting (26) into (27) and simplifying it, we have

$$
\xi(i) = \frac{\rho q(i)}{2+\mu} \coth\left(\frac{q(i)\rho}{2} \right). \tag{28}
$$

Hence by using the artificial viscosity into (23) and simplifying it, then we get

$$
\begin{aligned}
&\left[-\frac{\xi(i)(2+\mu)}{2h^2} - \frac{q_i}{2h} + \nu_i^{j+1}\frac{4-\mu}{24} \right] a_{i-1} + \left[\frac{\xi(2+\mu)}{2h^2} + \frac{8+\mu}{12} \right] a_i \\
&+ \left[-\frac{\xi(2+\mu)}{2h^2} - \frac{q_i}{2h} + \frac{4-\mu}{24}\nu_i^{j+1} \right] a_{i+1} = F_i^j.
\end{aligned}
\tag{29}
$$

Let

$$
\begin{aligned}
\mathfrak{H}_i^- &= -\frac{\xi(2+\mu)}{2h^2} - \frac{q_i}{2h} + \nu_i^{j+1}\frac{4-\mu}{24}, \\
\mathfrak{H}_i^0 &= \frac{\xi(2+\mu)}{2h^2} + \frac{8+\mu}{12}, \\
\mathfrak{H}_i^+ &= -\frac{\xi(2+\mu)}{2h^2} - \frac{q_i}{2h} + \frac{4-\mu}{24}\nu_i^{j+1}.
\end{aligned}
$$

Then

$$
\mathfrak{H}_i^- a_{i-1} + \mathfrak{H}_i^0 a_i + \mathfrak{H}_i^+ a_{i+1} = F_i^j. \tag{30}
$$

For the given boundary conditions, we have

$$
\begin{aligned}
\frac{4-\mu}{24}a_{-1} + \frac{8+\mu}{12}a_0 + \frac{4-\mu}{24}a_1 &= \varphi_l(t_{j+1}), \\
\frac{4-\mu}{24}a_{N_h-1} + \frac{8+\mu}{12}a_{N_h} + \frac{4-\mu}{24}a_{N_h+1} &= \varphi_r(t_{j+1}).
\end{aligned}
\tag{31}
$$

For $(N_h + 3) \times (N_h + 3)$ systems, (30)–(31) provide the $(N_h + 3)$ unknowns $a_{-1}, a_0, a_1, \ldots, a_{N_h+1}$. The (N_h+1) system of equations in (N_h+1) unknowns $a_0, a_1, \ldots, a_{N_h}$, can be expressed in the matrix form by eliminating a_{-1} and a_{N_h+1} from (30)–(31),

$$HA = F, \tag{32}$$

where

$$H = \begin{bmatrix} -2\left(\frac{8+\mu}{4-\mu}\right)\mathfrak{H}_0^- + \mathfrak{H}_0^0 & -\mathfrak{H}_0^- + \mathfrak{H}_0^+ & & & & \\ \mathfrak{H}_1^- & \mathfrak{H}_1^0 & \mathfrak{H}_1^+ & & & \\ \ddots & \ddots & \ddots & & & \\ & \mathfrak{H}_i^- & \mathfrak{H}_i^0 & \mathfrak{H}_i^+ & & \\ & & \ddots & \ddots & \ddots & \\ & & & \mathfrak{H}_{Nh-1}^- & \mathfrak{H}_{Nh-1}^0 & \mathfrak{H}_{Nh-1}^+ \\ & & & & \mathfrak{H}_{N_h}^- - \mathfrak{H}_{N_h}^+ & -2\left(\frac{8+\mu}{4-\mu}\right)\mathfrak{H}_{N_h}^- + \mathfrak{H}_{N_h}^0 \end{bmatrix},$$

$$A = \begin{bmatrix} a_0 & a_1 & \ldots & a_{N_h-1} & a_{N_h} \end{bmatrix}^T$$

and

$$F = \begin{bmatrix} F_0^j - \dfrac{24}{4-\mu}H_0^- \varphi_l(t_{j+1}) & F_1^j & F_2^j & \ldots & F_{N_h-1}^j & F_{N_h}^j - \dfrac{24}{4-\mu}H_{N_h}^- \varphi_r(t_{j+1}) \end{bmatrix}^T.$$

5 Convergence analysis

Lemma 7. Consider the extended cubic B-spline

$$G = \{G_{-1}(x,\mu), G_0(x,\mu), G_1(x,\mu), \ldots, G_{N_h}(x,\mu), G_{N_h+1}(x,\mu)\}$$

given in (19). It satisfies the inequality

$$\sum_{i=-1}^{N_h+1} |(G_i(x,\mu))| \leq \frac{7}{4}. \tag{33}$$

Proof. We start from the known properties

$$\left| \sum_{i=-1}^{N_h+1} G_i(x_i,\mu) \right| = \sum_{i=-1}^{N_h+1} |G_i(x_i,\mu)|,$$

where $G_i(x,\mu)$ is nonzero at three nodal points only. Thus, using Table 1, at every nodal value x_i, we obtain

$$\sum_{i=-1}^{N_h+1} |G_i(x_i,\mu)| = |G_{i-1}(x_i,\mu)| + |G_i(x_i,\mu)| + |G_{i+1}(x_i,\mu)|$$

$$= \frac{4-\mu}{24} + \frac{8+\mu}{12} + \frac{4-\mu}{24} = 1 < \frac{7}{4}.$$

From Table 1, for $x_{i-1} \le x \le x_i$, we have

$$|G_i(x_i,\mu)| \le \frac{8+\mu}{12}, \quad |G_{i-1}(x_i,\mu)| \le \frac{8+\mu}{12}.$$

Similarly, for $x_{i-1} \le x \le x_i$, we get

$$|G_{i+1}(x_i,\mu)| \le \frac{8+\mu}{12}, \quad |G_{i-2}(x_i,\mu)| \le \frac{8+\mu}{12}.$$

Now, for any point $x \in [x_{i-1}, x_i]$, we obtain

$$\sum_{i=-1}^{N_h+1} |G_i(x_i,\mu)| = |G_{i-1}(x_i,\mu)| + |G_i(x_i,\mu)| + |G_{i+1}(x_i,\mu)|$$

$$= \frac{4-\mu}{24} + \frac{8+\mu}{12} + \frac{4-\mu}{24} = \frac{20-\mu}{12}.$$

Since $-8 < \mu < 1$, thus

$$\sum_{i=-1}^{N_h+1} |G_i(x_i,\mu)| = \frac{20-\mu}{12} < \frac{7}{4}.$$

$\square$

Let $\bar\Psi$ be a unique cubic spline interpolate obtained from an approximately solution $Y(x,\mu)$ of the problems (11) to the given solution $y(x)$. Then

$$\bar\psi(x) = \sum_{i=-1}^{N_h+1} \bar{A} G_i(x,\mu). \tag{34}$$

For $z > 0$, let $\alpha(z) = z\coth(z)$ satisfy $\alpha(0) = 1, \alpha(z) = \alpha(-z)$. Then $|\alpha(z) - 1| \le Cz^2$ for $0 < z \le 1$. Since $\coth z \longrightarrow 1$ as $z \longrightarrow \infty$, so $|\alpha(z) - 1| \le Cz$. Hence for $z > 0$, we have

$$|\xi(z) - 1| \le \frac{Cz^2}{1+z} \quad \text{and} \quad \frac{\varepsilon(h/\varepsilon)^2}{h/\varepsilon + 1} = \frac{h^2}{h+\varepsilon}. \tag{35}$$

Lemma 8. Set a cubic spline interpolant $\bar\Psi \in C^2(0,1)$ to a solution $Y(x)$. For $x \in (x_i, x_{i+1})$, the standard cubic spline interpolation approximate holds

if $Y(x) \in C^4(0,1)$. According to Hall's estimate [20], we have

$$\left| Y^{(}k)(x) - \bar{\Psi}(x)^{(k)} \right| \leq c_i \left\| Y^{(4)} \right\| N_h^{-(4-k)}, \tag{36}$$

where c_i's are constants independent of h and N_h.

Theorem 2. [Parameter uniform convergence] Let $S(x, \mu)$ be the collocation approximation from the space of splines to the solution, $Y^{j+1}(x)$ be the approximate solution of the semi-discretized problem (11), and let $y(x_i, t_{j+1})$ be the continuous solution of (1) and (2). Therefore, the following error bound is valid for suitably large N:

$$\left\| Y^{j+1}(x_i) - y^{j+1}(x_i) \right\| \leq \frac{N_h^{-2}}{N_h^{-1} + \varepsilon}. \tag{37}$$

Proof. To prove the theorem, we start by using Lemma 5. We get the bounds

$$
\begin{aligned}
\left| Y^{j+1}(x_i) - \bar{\Psi}(x_i) \right| &\leq c_0 \left\| \frac{d^4 Y^{j+1}(x_i)}{dx^4} \right\| N_h^{-4}, \\
\left| \frac{dY^{j+1}(x_i)}{dx} - \frac{d\bar{\Psi}(x_i)}{dx} \right| &\leq c_1 \left\| \frac{d^4 Y^{j+1}(x_i)}{dx^4} \right\| N_h^{-3}, \\
\left| \frac{d^2 Y^{j+1}(x_i)}{dx^2} - \frac{d^2 \bar{\Psi}(x_i)}{dx^2} \right| &\leq c_2 \left\| \frac{d^4 Y^{j+1}(x_i)}{dx^4} \right\| N_h^{-2}.
\end{aligned} \tag{38}
$$

Using the triangle inequality, we have

$$\left| Y^{j+1}(x_i) - y^{j+1}(x_i) \right| \leq \left| Y^{j+1}(x_i) - \bar{\Psi}(x_i) \right| + \left| \bar{\Psi}(x_i) - y^{j+1}(x_i) \right|.$$

The collocating condition gives

$$\tilde{\mathfrak{L}}_\varepsilon^{h,\tau} y^{j+1}(x_i) = \tilde{\mathfrak{L}}_\varepsilon^{h,\tau} Y^{j+1}(x_i).$$

Assume that $\tilde{\mathfrak{L}}_\varepsilon^{h,\tau} \bar{\Psi}(x_i) = \bar{F}(x_i, t_j)$, which satisfies the boundary conditions, $\bar{\Psi}(x_0) = \bar{\Psi}(x_{N_h+1})$. Then

$$
\begin{aligned}
\left| \tilde{\mathfrak{L}}_\varepsilon^{h,\tau} y^{j+1}(x_i) - \tilde{\mathfrak{L}}_\varepsilon^{h,\tau} \bar{\Psi}(x_i) \right| &= \left| \tilde{\mathfrak{L}}_\varepsilon^{h,\tau} Y^{j+1}(x_i) - \tilde{\mathfrak{L}}_\varepsilon^{h,\tau} \bar{\Psi}(x_i) \right| \\
&= \left| -\varepsilon \left(\frac{d^2 y^{j+1}(x_i)}{dx^2} - \xi_i(\varepsilon) \frac{d^2 \bar{\Psi}(x_i)}{dx^2} \right) \right| \\
&\quad + \left| q(x_i) \left(\frac{dy^{j+1}(x_i)}{dx} - \frac{d\bar{\Psi}(x_i)}{dx} \right) \right|
\end{aligned}
$$

$$+ \left| \nu^{j+1}(x-i)(y^{j+1}(x_i) - \bar{\Psi}(x_i)) \right|$$

$$\leq |\varepsilon|\,|\xi| \left\| \frac{d^2 y^{j+1}(x_i)}{dx^2} \right\|$$

$$+ |\varepsilon|\,|\xi| \left| \frac{d^2 y^{j+1}(x_i)}{dx^2} - \xi_i(\varepsilon)\frac{d^2 \bar{\Psi}(x_i)}{dx^2} \right|$$

$$+ |q(x_i)| \left| \frac{dy^{j+1}(x_i)}{dx} - \frac{d\bar{\Psi}(x_i)}{dx} \right|$$

$$+ \left| \nu^{j+1} \right| \left| y^{j+1}(x_i) - \bar{\Psi}(x_i) \right|. \tag{39}$$

Now, using (35) and Lemma 1, then we obtain

$$\max_{0 \leq i,j \leq N_h, M_\tau} \left| y^{j+1}(x_i) - \bar{\Psi}(x_i) \right| \leq \frac{N_h^{-2}}{N_h^{-1} + \varepsilon}$$

$$\Rightarrow \left\| y^{j+1}(x_i) - \bar{\Psi}(x_i) \right\| \leq \frac{N_h^{-2}}{N_h^{-1} + \varepsilon}. \tag{40}$$

The coefficient matrix associated with (20) is of size $(N_h + 1) \times (N_h + 1)$ with its elements. For $i = 1, 2, \ldots, N_h - 1$, we have

$$\mathfrak{H}_i^- < 0, \quad \text{since} \quad \text{all} \quad \text{terms} \quad \text{are positive},$$

$$\mathfrak{H}_i^0 > 0, \quad \text{since} \quad \text{all} \quad \text{terms} \quad \text{are positive},$$

$$\mathfrak{H}_i^+ < 0, \quad \text{since} \quad \text{all} \quad \text{terms} \quad \text{are positive} \quad \coth\left(\frac{q(i)\varepsilon}{2h}\right) \geq 1.$$

Thus, the coefficient matrix of the proposed method, satisfies the properties of M-matrix. This implies that the inverse matrix exists and it is nonnegative. This implies [40]

$$\left| H^{-1} \right| < C N_h^{-2}. \tag{41}$$

From (32) and $\mathfrak{L}_\varepsilon^{h,\tau} y^{j+1}(x_i) - \tilde{\mathfrak{L}}_\varepsilon^{h,\tau} \bar{\Psi}(x_i)$, we get the result

$$H(A - \bar{A}) = F - \bar{F}, \tag{42}$$

where $A - \bar{A} = (a_0 - \bar{a}_0, \quad a_1 - \bar{a}_1, \quad a_2 - \bar{a}_2, \ldots, \quad a_{N_h} - \bar{a}_{N_h})$ and $F - \bar{F} = \left(F(x_0, t_j) - \bar{F}(x_0, t_j), \quad F(x_1, t_j) - \bar{F}(x_1, t_j), \ldots, F(x_{N_h}, t_j) - \bar{F}(x_{N_h}, t_j)\right)$. Using (41), so the boundary conditions are bounded. Therefore, (39) and (42) give

$$\left| A - \bar{A} \right| \leq \frac{N_h^{-2}}{N_h^{-1} + \varepsilon}.$$

Hence, by using (21) for $Y(x, \mu)$ and Lemma 34 for $\bar{\Psi}(x)$, we get

$$\left|Y(x_i, \mu) - \bar{\Psi}(x_i)\right| = \left|A - \bar{A}\right| \sum_0^{N_h+1} \left|G_i(x_i, \mu)\right| \leq \frac{N_h^{-2}}{N_h^{-1} + \varepsilon}. \qquad (43)$$

Thus, using (40) and (43), also the triangle inequality, we obtain our result

$$\left\|Y^{j+1}(x_i) - y^{j+1}(x_i)\right\| \leq \frac{N_h^{-2}}{N_h^{-1} + \varepsilon}. \qquad (44)$$

$\square$

Theorem 3. If y and Y be exact and cubic B-spline approximation solution of the problem (1), respectively, then the following error bound holds:

$$\max_{0 \leq i,j \leq M_h, M_t} |y(x_i, t_j) - Y(x_i, \mu)| \leq C \left(\frac{h^2}{h + \varepsilon} + (\tau)^{2-\gamma} \right). \qquad (45)$$

Proof. By combining Theorems 6 and 2, we get our result. $\square$

6 Numerical result

In this section, we show two numerical examples that demonstrate the accuracy of the method and the result of the error analysis. Separate tables display the error and corresponding convergence rates for each of these two test examples. Since the exact solution to the example is unknown, double mesh will be used in this article to determine the accuracy of the numerical solution. The maximum point-wise absolute error is determined as

$$E_\varepsilon^{N_h, M_\tau} = \max_{0 \leq i,j \leq N_h, M_\tau} \left| Y_{i,j}^{N_h, M_\tau}(x_i, t_j) - Y_{i,j}^{2N_h, 2M_\tau}(x_{2i}, t_{2j}) \right|,$$

where N_h and M_τ are the number of mesh points in the spatial and temporal directions, respectively. The parameter uniform error estimation is defined as

$$e^{N_h, M_\tau} = \max_\varepsilon \{E_\varepsilon^{N_h, M_\tau}\}.$$

Next, we also determine the rate of convergence of the method by using the formula

$$RoC_\varepsilon^{N_h, M_\tau} = \log_2 \left(\frac{E_\varepsilon^{N_h, M_\tau}}{E_\varepsilon^{2N_h, 2M_\tau}} \right).$$

The parameter uniform rate of convergence is defined as

$$R^{N_h, M_\tau} = \max_\varepsilon \{ RoC_\varepsilon^{N_h, M_\tau} \}.$$

Example 1. Consider the time-fractional SPPPDE

$$D_t^\gamma y(x,t) - \varepsilon \frac{\partial^2 y(x,t)}{\partial x^2} + \left(2 - x^2\right) \frac{\partial y(x,t)}{\partial x} + ((x+1)(t+1))y(x,t)$$

$$= y(x, t-1) + 10t^2 \exp(-t)x(1-x),$$

on $(x,t) \in \Omega = (0,1) \times (0, \mathfrak{T}]$, with initial and boundary conditions $\varphi_b(x,t) = 0$, $\varphi_l(t) = 0$ and $\varphi_r(t) = 0$.

(a) $\varepsilon = 2^0$

(b) $\varepsilon = 2^{-6}$

(c) $\varepsilon = 2^{-10}$

(d) $\varepsilon = 2^{-20}$
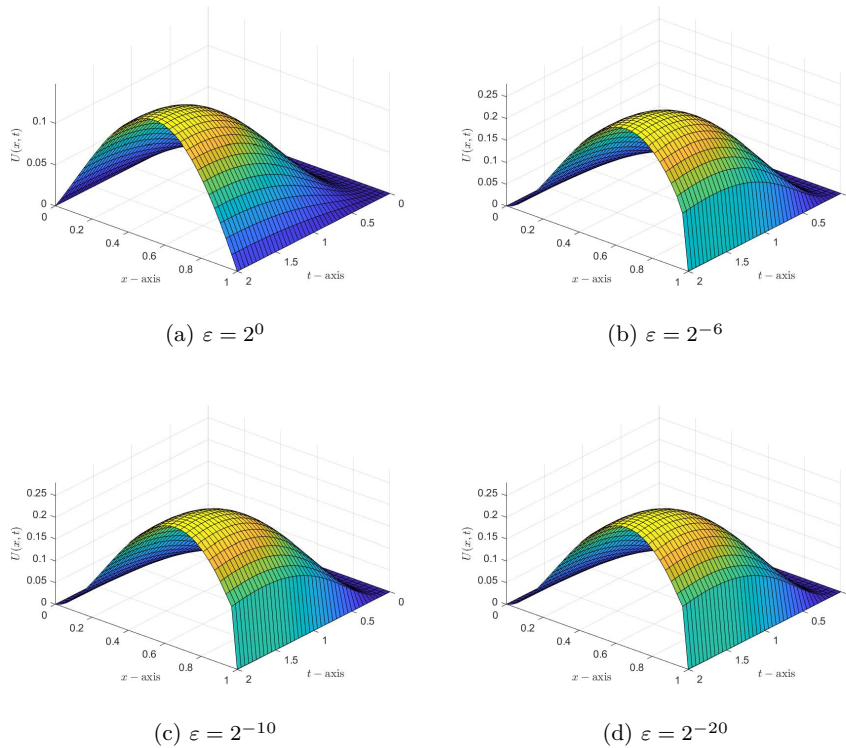
Figure 1: Three-dimensional plot of the numerical solution for Example 1 for different values of ε with $\gamma = 0.5, N_h = 32$, and $M_\tau = 40$.

Table 2: Absolute maximum error and rate of convergence for Example 1 for different values of ε, with fix $\gamma = 0.5$

$(N_h, M_\tau) \Rightarrow$	(16,20)	(32,40)	(64,80)	(128, 160)	(256, 320)	(512, 400)
$\varepsilon = 2^0$	4.1605e-03	1.9136e-03	8.5272e-04	3.6840e-04	1.5434e-04	6.2758e-05
	1.1205	1.1662	1.2108	1.2551	1.2983	-
$\varepsilon = 2^{-2}$	7.8335e-03	3.3678e-03	1.3897e-03	5.5457e-04	2.1515e-04	8.1537e-05
	1.2179	1.2771	1.3253	1.3661	1.3998	-
$\varepsilon = 2^{-4}$	9.5332e-03	3.9931e-03	1.6048e-03	6.2416e-04	2.3637e-04	8.7649e-05
	1.2554	1.3151	1.3624	1.4009	1.4312	-
$\varepsilon = 2^{-6}$	9.8688e-03	4.1357e-03	1.6591e-03	6.4279e-04	2.4217e-04	8.9302e-05
	1.2548	1.3177	1.3680	1.4083	1.4393	-
$\varepsilon = 2^{-8}$	9.8893e-03	4.1566e-03	1.6705e-03	6.4735e-04	2.4366e-04	8.9726e-05
	1.2505	1.3151	1.3676	1.4097	1.4413	-
$\varepsilon = 2^{-10}$	9.8893e-03	4.1568e-03	1.6711e-03	6.4798e-04	2.4397e-04	8.9826e-05
	1.2504	1.3147	1.3668	1.4093	1.4415	-
$\varepsilon = 2^{-12}$	9.8893e-03	4.1568e-03	1.6711e-03	6.4798e-04	2.4398e-04	8.9840e-05
	1.2504	1.3147	1.3668	1.4092	1.4414	-
$\varepsilon = 2^{-14}$	9.8893e-03	4.1568e-03	1.6711e-03	6.4798e-04	2.4398e-04	8.9840e-05
	1.2504	1.3147	1.3668	1.4092	1.4414	-
$\varepsilon = 2^{-20}$	9.8893e-03	4.1568e-03	1.6711e-03	6.4798e-04	2.4398e-04	8.9840e-05
	1.2504	1.3147	1.3668	1.4092	1.4414	-
$\varepsilon = 2^{-25}$	9.8893e-03	4.1568e-03	1.6711e-03	6.4798e-04	2.4398e-04	8.9840e-05
	1.2504	1.3147	1.3668	1.4092	1.4414	-
$\varepsilon = 2^{-30}$	9.8893e-03	4.1568e-03	1.6711e-03	6.4798e-04	2.4398e-04	8.9840e-05
	1.2504	1.3147	1.3668	1.4092	1.4414	-
e^{N_h, M_τ}	9.8893e-03	4.1568e-03	1.6711e-03	6.4798e-04	2.4398e-04	8.9840e-05
R^{N_h, M_τ}	1.2504	1.3147	1.3668	1.4092	1.4414	-

Table 3: Comparison of absolute maximum error and rate of convergence for Example 1 for different values of ε, with fix $\gamma = 0.5$

$(N_h, M_\tau) \Rightarrow$	(16,20)	(32,40)	(64,80)	(128, 160)
		Proposed Method		
$\varepsilon = 2^{-6}$	9.8688e-03	4.1357e-03	1.6591e-03	6.4279e-04
	1.2548	1.3177	1.3680	-
$\varepsilon = 2^{-8}$	9.8893e-03	4.1566e-03	1.6705e-03	6.4735e-04
	1.2505	1.3151	1.3676	-
$\varepsilon = 2^{-10}$	9.8893e-03	4.1568e-03	1.6711e-03	6.4798e-04
	1.2504	1.3147	1.3668	-
$\varepsilon = 2^{-12}$	1.4000e-02	5.5760e-03	2.1233e-03	7.8272e-04
	1.3281	1.3929	1.4398	-
$\varepsilon = 2^{-14}$	1.4000e-02	5.5760e-03	2.1233e-03	7.8272e-04
	1.3281	1.3929	1.4398	-
$\varepsilon = 2^{-20}$	9.8893e-03	4.1568e-03	1.6711e-03	6.4798e-04
	1.2504	1.3147	1.3668	-
$\varepsilon = 2^{-25}$	9.8893e-03	4.1568e-03	1.6711e-03	6.4798e-04
	1.2504	1.3147	1.3668	-
$\varepsilon = 2^{-30}$	9.8893e-03	4.1568e-03	1.6711e-03	6.4798e-04
	1.2504	1.3147	1.3668	-
e^{N_h, M_τ}	9.8893e-03	4.1568e-03	1.6711e-03	6.4798e-04
R^{N_h, M_τ}	1.2504	1.3147	1.3668	-
		Method in reference [27]		
$\varepsilon = 2^{-6}$	1.0088E-02	4.9401e-03	2.0143e-03	7.1385E-04
	1.0300	1.2943	1.4966	-
$\varepsilon = 2^{-8}$	1.1863e-02	6.3546e-03	3.3404e-03	1.8221e-03
	0.9006	0.9278	0.8744	-
$\varepsilon = 2^{-10}$	1.2246e-02	6.6457e-03	3.4625e-03	1.7661e-03
	0.8818	0.9406	0.9712	-
$\varepsilon = 2^{-12}$	1.2336e-02	6.7141e-03	3.5082e-03	1.7930e-03
	0.8776	0.9365	0.9683	-
$\varepsilon = 2^{-20}$	1.2365e-02	6.7364e-03	3.5230e-03	1.8022e-03
	0.8762	0.9352	0.9670	-
$\varepsilon = 2^{-25}$	1.2365e-02	6.7364e-03	3.5230e-03	1.8022e-03
	0.8762	0.9352	0.9670	-
$\varepsilon = 2^{-30}$	1.2365e-02	6.7364e-03	3.5230e-03	1.8022e-03
	0.8762	0.9352	0.9670	-
e^{N_h, M_τ}	1.2365e-02	6.7364e-03	3.5230e-03	1.8022e-03
R^{N_h, M_τ}	0.8762	0.9352	0.9670	-

Example 2. Consider the time-fractional SPPPDE

$$D_t^\gamma y(x,t) - \varepsilon \frac{\partial^2 y(x,t)}{\partial x^2} + \left(2 - x^2\right) \frac{\partial y(x,t)}{\partial x} + xy(x,t)$$
$$= y(x,t-1) + 10t^2 \exp(-t)x(1-x),$$

on $(x,t) \in \Omega = (0,1) \times (0,\mathfrak{T}]$, with initial and boundary conditions $\varphi_b(x,t) = 0$, $\varphi_l(t) = 0$ and $\varphi_r(t) = 0$.

(a) $\varepsilon = 2^0$

(b) $\varepsilon = 2^{-6}$

(c) $\varepsilon = 2^{-10}$

(d) $\varepsilon = 2^{-20}$
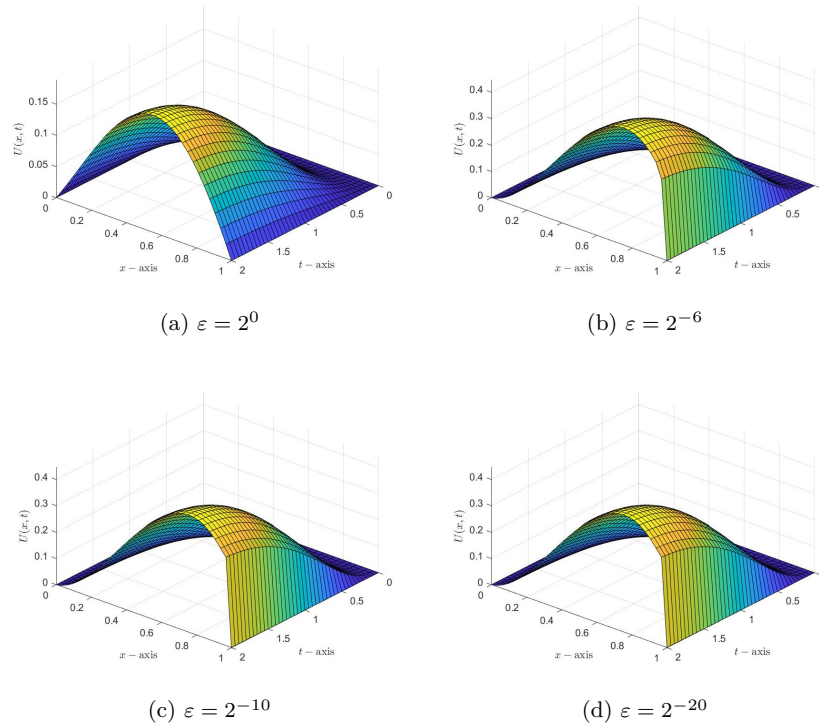
Figure 2: Three-dimensional plot of the numerical solution for Example 2 for different values of ε with $\gamma = 0.5, M_x = 32$, and $M_t = 40$.

The numerical results are described in terms of maximum absolute errors and numerical rate of convergence in Tables 2 and 4. These results are compared with those of a previously developed numerical approach found in the literature in [27], using Tables 3 and 5. Additionally, the log-log plot (Figure 3) and the numerical solution for Examples 1 and 2 (refer to Figures

Table 4: Maximum error and rate of convergence for Example 2 for different values of ε, with fix $\gamma = 0.5$

$(N_h, M_\tau) \Rightarrow$	(16,20)	(32,40)	(64,80)	(128, 160)	(256, 320)	(512, 400)
$\varepsilon = 2^0$	5.0614e-03	2.2923e-03	1.0036e-03	4.2492e-04	1.7424e-04	6.9357e-05
	1.1427	1.1916	1.2400	1.2861	1.3290	-
$\varepsilon = 2^{-2}$	1.1193e-02	4.6126e-03	1.8150e-03	6.8997e-04	2.5570e-04	9.3106e-05
	1.2789	1.3456	1.3954	1.4321	1.4575	-
$\varepsilon = 2^{-4}$	1.4655e-02	5.8083e-03	2.1878e-03	7.9856e-04	2.8584e-04	1.0112e-04
	1.3352	1.4087	1.4540	1.4822	1.4992	-
$\varepsilon = 2^{-6}$	1.5546e-02	6.0863e-03	2.2785e-03	8.2711e-04	2.9408e-04	1.0330e-04
	1.3529	1.4175	1.4620	1.4919	1.5094	-
$\varepsilon = 2^{-8}$	1.5610e-02	6.1249e-03	2.2975e-03	8.3410e-04	2.9620e-04	1.0386e-04
	1.3497	1.4146	1.4618	1.4937	1.5119	-
$\varepsilon = 2^{-10}$	1.5610e-02	6.1253e-03	2.2986e-03	8.3507e-04	2.9663e-04	1.0399e-04
	1.3496	1.4140	1.4608	1.4932	1.5122	-
$\varepsilon = 2^{-12}$	1.5610e-02	6.1253e-03	2.2986e-03	8.3507e-04	2.9666e-04	1.0401e-04
	1.3496	1.4140	1.4608	1.4931	1.5121	-
$\varepsilon = 2^{-14}$	1.5610e-02	6.1253e-03	2.2986e-03	8.3507e-04	2.9666e-04	1.0401e-04
	1.3496	1.4140	1.4608	1.4931	1.5121	-
$\varepsilon = 2^{-20}$	1.5610e-02	6.1253e-03	2.2986e-03	8.3507e-04	2.9666e-04	1.0401e-04
	1.3496	1.4140	1.4608	1.4931	1.5121	-
$\varepsilon = 2^{-30}$	1.5610e-02	6.1253e-03	2.2986e-03	8.3507e-04	2.9666e-04	1.0401e-04
	1.3496	1.4140	1.4608	1.4931	1.5121	-
e^{N_h, M_τ}	1.5610e-02	6.1253e-03	2.2986e-03	8.3507e-04	2.9666e-04	1.0401e-04
R^{N_h, M_τ}	1.3496	1.4140	1.4608	1.4931	1.5121	-

1 and 2) demonstrate the ε-uniform convergence of the scheme. A boundary layer, as shown in Figures 1 and 2, is located at the right side of the space domain in the numerical solution of Examples 1 and 2 above. Figures 1 and 2 also display the computed solutions $y_{i,j}$ for various perturbation parameter values, along with the influence of fractional order. Figure 3 displays the log-log plots of the maximum absolute errors against the number of meshes for both cases, demonstrating the developed numerical scheme's convergent nature regardless of the perturbation value. The suggested scheme is ε-uniformly convergent, as illustrated by the numerical results shown in Tables 2 and 4, by combining extended cubic B-spline collocation with artificial viscosity numerical method in the spatial direction with the implicit Euler's method in the temporal direction. We can see that, for each value of ε, the

Table 5: Comparison of maximum error and rate of convergence for Example 2 for different values of ε, with fix $\gamma = 0.5$

$(N_h, M_\tau) \Rightarrow$	(16,20)	(32,40)	(64,80)	(128, 160)
		Proposed Method		
$\varepsilon = 2^{-6}$	1.5546e-02	6.0863e-03	2.2785e-03	8.2711e-04
	1.3529	1.4175	1.4620	-
$\varepsilon = 2^{-8}$	1.5610e-02	6.1249e-03	2.2975e-03	8.3410e-04
	1.3497	1.4146	1.4618	-
$\varepsilon = 2^{-10}$	1.5610e-02	6.1253e-03	2.2986e-03	8.3507e-04
	1.3496	1.4140	1.4608	-
$\varepsilon = 2^{-12}$	1.5610e-02	6.1253e-03	2.2986e-03	8.3507e-04
	1.3496	1.4140	1.4608	-
$\varepsilon = 2^{-14}$	1.5610e-02	6.1253e-03	2.2986e-03	8.3507e-04
	1.3496	1.4140	1.4608	-
$\varepsilon = 2^{-20}$	1.5610e-02	6.1253e-03	2.2986e-03	8.3507e-04
	1.3496	1.4140	1.4608	-
$\varepsilon = 2^{-30}$	1.5610e-02	6.1253e-03	2.2986e-03	8.3507e-04
	1.3496	1.4140	1.4608	-
e^{N_h, M_τ}	1.5610e-02	6.1253e-03	2.2986e-03	8.3507e-04
R^{N_h, M_τ}	1.3496	1.4140	1.4608	-
		Method in reference ([27])		
$\varepsilon = 2^{-6}$	1.5818e-02	7.8811e-03	2.9140e-03	8.1121E-04
	1.0051	1.4354	1.8449	-
$\varepsilon = 2^{-8}$	2.1516e-02	9.5195e-03	4.7373e-03	2.2942e-03
	1.1765	1.0068	1.0461	
$\varepsilon = 2^{-10}$	2.4877e-02	1.1527e-02	5.4771e-03	2.6471e-03
	1.1098	1.0735	1.0490	-
$\varepsilon = 2^{-12}$	2.5768e-02	1.2070e-02	5.7971e-03	2.8303e-03
	1.0942	1.0580	1.0344	-
$\varepsilon = 2^{-15}$	2.6068e-02	1.2257e-02	5.9063e-03	2.8933e-03
	1.0887	1.0533	1.0295	-
$\varepsilon = 2^{-25}$	2.6069e-02	1.2258e-02	5.9068e-03	2.8935e-03
	1.0886	1.0533	1.0296	-
$\varepsilon = 2^{-30}$	2.6069e-02	1.2258e-02	5.9068e-03	2.8935e-03
	1.0886	1.0533	1.0296	-
e^{N_h, M_τ}	2.6069e-02	1.2258e-02	5.9068e-03	2.8935e-03
R^{N_h, M_τ}	1.0886	1.0533	1.0296	-

(a) Log-log plot of the max error for Example 1

(b) Log-log plot of the max error for Example 2
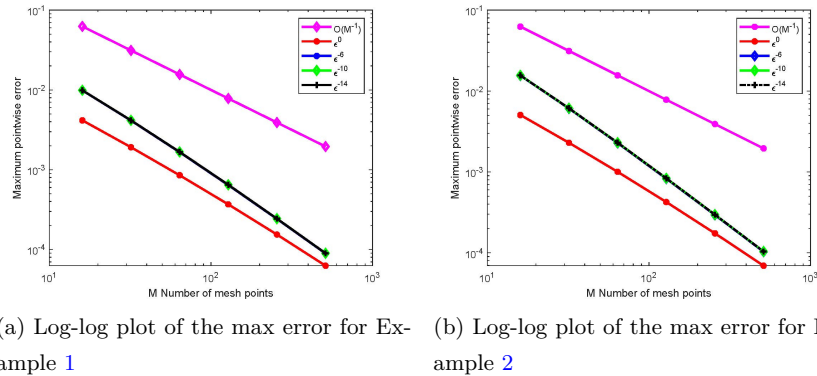
Figure 3: Log-log plot of maximum absolute errors for Examples 1 and 2 for different values of ε.

maximum point-wise error decreases as N_h, M_τ grows from the results in Tables 2 and 4. It is evident that, for every N_h, M_τ, the maximum point-wise error is $\varepsilon \longrightarrow 0$ stable. By utilizing these two examples, we verify that the suggested numerical technique is more accurate, stable, and ε-uniformly convergent, with a convergence rate that is almost one. The execution of the proposed method is done by using the MATLAB R2022b software package.

7 Conclusion

We solved the time delay singularly perturbed parabolic convection-diffusion problem with the time-fractional order of derivative using the extended cubic B-spline collocation method. The solution to the problem showed a boundary layer on the right side of the spatial domain. The layer region of the solution has a steep gradient due to the existence of ε. Because of the rapidly changing solution behavior in the layer region, it is computationally challenging to determine the solution analytically or using standard numerical approaches. To control this effect, we came up with a plan that makes use of an extended cubic B-spline collocation scheme in the spatial direction and an implicit Euler's scheme in the temporal direction. It has been demonstrated that the developed numerical approach is stable and converges uniformly.

Two model problems have been taken into consideration for the numerical experimentation for various values of the perturbation parameter and fractional order derivatives in order to confirm the method's compatibility. The scheme was shown to have an order of convergence of $O(\frac{N_h^{-2}}{N_h^{-1}+1} + \tau^{2-\gamma})$ and to be ε-uniformly convergent.

Acknowledgements

References

[1] Abel, N.H. *œuvres complètes de Niels Henrik Abel*, Vol. 1. Cambridge University Press, 2012.

[2] Al-Mdallal, Q.M. and Syam, M.I. *An efficient method for solving nonlinear singularly perturbed two points boundary-value problems of fractional order*, Commun. Nonlinear Sci. Numer. Simul. 17(6) (2012), 2299–2308.

[3] Anilay, W.T., Duressa, G.F. and Woldaregay, M.M. *Higher order uniformly convergent numerical scheme for singularly perturbed reaction-diffusion problems*, Kyungpook Math. J. 61(3) (2021), 591–612.

[4] Atangana, A. and Doungmo Goufo, E.F. *Extension of matched asymptotic method to fractional boundary layers problems*, Math. Probl. Eng. 2014(1) (2014), 107535.

[5] Bijura, A.M. *Nonlinear singular perturbation problems of arbitrary real orders*, No. IC–2003/130, Trieste; Italy, The Abdus Salam International Center for Theoretical Physics, 2003.

[6] Choudhary, R., Singh, S. and Kumar, D. *A second-order numerical scheme for the time-fractional partial differential equations with a time delay,* Comput. Appl. Math. 41(3) (2022), 1–28.

[7] Cooke, K.L. *Differential—difference equations,* In International symposium on nonlinear differential equations and nonlinear mechanics, Elsevier, 1963, 155–171.

[8] Daba, I.T. and Duressa, G.F. *Extended cubic b-spline collocation method for singularly perturbed parabolic differential-difference equation arising in computational neuroscience,* Int. J. Numer. Methods Biomed. Eng. 37(2) (2021), e3418.

[9] Daba, I.T. and Duressa, G.F. *Collocation method using artificial viscosity for time dependent singularly perturbed differential–difference equations,* Math. Comput. Simul. 192 (2022), 201–220.

[10] Dağ, İ.D.R.İ.S., Irk, D.U.R.S.U.N. and Sarı, M. *The extended cubic b-spline algorithm for a modified regularized long wave equation,* Chinese Physics B 22(4) (2013), 040207.

[11] Diekmann, O., Van Gils, S.A., Lunel, S.M. and Walther, H.O. *Delay equations: functional-, complex-, and nonlinear analysis,* volume 110. Springer Science & Business Media, 2012.

[12] Driver, R.D. *Ordinary and delay differential equations,* volume 20. Springer Science & Business Media, 2012.

[13] Farrell, P., Hegarty, A., Miller, J.M., O'Riordan, E. and Shishkin, G.I. *Robust computational techniques for boundary layers,* Chapman and hall/CRC, 2000.

[14] Gelu, F.W. and Duressa, G.F. *Hybrid method for singularly perturbed robin type parabolic convection–diffusion problems on Shishkin mesh,* Partial Differ. Equ. Appl. Math. 8 (2023), 100586.

[15] Gerasimov, A.N. *A generalization of linear laws of deformation and its application to problems of internal friction,* Akad. Nauk SSSR. Prikl. Mat. Meh 12(3) (1948), 251–260.

[16] Hailu, W.S. and Duressa, G.F. *Accelerated parameter-uniform numerical method for singularly perturbed parabolic convection-diffusion problems with a large negative shift and integral boundary condition*, Results Appl. Math. 18 (2023), 100364.

[17] Hailu, W.S. and Duressa, G.F. *Uniformly convergent numerical scheme for solving singularly perturbed parabolic convection-diffusion equations with integral boundary condition*, Differ. Equ. Dyn. Syst. (2023), 1–27.

[18] Hailu, W.S. and Duressa, G.F. *A robust collocation method for singularly perturbed discontinuous coefficients parabolic differential difference equations*, Res. Math. 11(1) (2024), 2301827.

[19] Hale, J.K. and Lunel, S.M.V. *Introduction to functional differential equations*, volume 99. Springer Science and Business Media, 2013.

[20] Hall, C.A. *On error bounds for spline interpolation*, J. Approx. Theory 1(2) (1968), 209–218.

[21] Kaslik, E. and Sivasundaram, S. *Analytical and numerical methods for the stability analysis of linear fractional delay differential equations*, J. Comput. Appl. Math. 236(16) (2012), 4027–4041.

[22] Kolmanovskii, V. and Myshkis, A. *Applied theory of functional differential equations*, volume 85. Springer Science and Business Media, 2012.

[23] Kolmanovskii, V.B. and Nosov, V.R. *Stability of functional differential equations*, volume 180, Elsevier, 1986.

[24] Kuang, Y. *Delay differential equations: with applications in population dynamics*, Academic press, 1993.

[25] Kumar, D. *A parameter-uniform scheme for the parabolic singularly perturbed problem with a delay in time*, Numer. Methods Partial Differ. Equ. 37(1) (2021), 626–642.

[26] Kumar, D. and Kadalbajoo, M.K. *A parameter-uniform numerical method for time-dependent singularly perturbed differential-difference equations*, Appl. Math. Model. 35(6) (2011), 2805–2819.

[27] Kumar, K., P, P.C. and Vigo-Aguiar, J. *Numerical solution of time-fractional singularly perturbed convection–diffusion problems with a delay in time*, Mathematical Methods in the Applied Sciences, 44(4) (2021), 3080–3097.

[28] Miller, J.J., O'riordan, E. and Shishkin, G.I. *Fitted numerical methods for singular perturbation problems: error estimates in the maximum norm for linear problems in one and two dimensions*, World scientific, 1996.

[29] Miller, K.S. and Ross, B. *An introduction to the fractional calculus and fractional differential equations*, Willey New York, 1993.

[30] Negero, N.T. and Duressa, G.F. *A method of line with improved accuracy for singularly perturbed parabolic convection–diffusion problems with large temporal lag*, Results Appl. Math. 11(2021), 100174.

[31] Negero, N.T. and Duressa, G.F. *Uniform convergent solution of singularly perturbed parabolic differential equations with general temporal-lag*, Iran. J. Sci. Technol. Trans. A: Sci. 46(2) (2022), 507–524.

[32] Nelson, P.W. and Perelson, A.S. *Mathematical analysis of delay differential equation models of HIV-1 infection*, Math. Biosci. 179(1) (2002), 73–94.

[33] Norkin, S.B. *Introduction to the theory and application of differential equations with deviating arguments*, Academic Press, 1973.

[34] O'malley, R.E. *Singular perturbation methods for ordinary differential equations*, volume 89. Springer, 1991.

[35] Prabhakar, T.R. *A singular integral equation with a generalized Mittag Leffler function in the kernel*, Yokohama Math. J. 19(1) (1971), 7–15.

[36] Roop, J.P. *Numerical approximation of a one-dimensional space fractional advection–dispersion equation with boundary layer*, Comput. Math. Appl. 56(7) (2008), 1808–1819.

[37] Sahoo, S.K. and Gupta, V. *A robust uniformly convergent finite difference scheme for the time-fractional singularly perturbed convection-diffusion problem*, Comput. Math. Appl. 137 (2023), 126–146.

[38] Sayevand, K. and Pichaghchi, K. *Efficient algorithms for analyzing the singularly perturbed boundary value problems of fractional order*, Commun. Nonlinear Sci. Numer. Simul. 57 (2018), 136–168.

[39] Sayevand, K. and Pichaghchi, K. *A novel operational matrix method for solving singularly perturbed boundary value problems of fractional multi-order*, Int. J. Comput. Math. 95(4) (2018), 767–796.

[40] Varah, J.M. *A lower bound for the smallest singular value of a matrix*, Linear Algebra Appl. 11(1) (1975), 3–5.

[41] Villasana, M. and Radunskaya, A. *A delay differential equation model for tumor growth*, J. Math. Biol. 47 (2003), 270–294.

[42] Xu, G., Wang, G.Z. and Chen, X.D. *Free-form deformation with rational dms-spline volumes*, J. Comput. Sci. Technol. 23(5) (2008), 862–873,

[43] Xuli, H. *An extension of the cubic uniform b-spline curve*, Journal of Computer Aided Design and Computer Graphics 15(5) (2003), 576–578.

[44] Zhao, T. *Global periodic-solutions for a differential delay system modeling a microbial population in the chemostat*, J. Math. Anal. Appl. 193(1) (1995), 329–352.